FOURTH EUROPEAN ROTORCRAFT AND POWERED LIFT AIRCRAFT FORUM

Paper No. 12

UNSTEADY AERODYNAMICS OF A CIRCULATION CONTROLLED AIRFOIL

L.V. SCHMIDT

Department of Aeronautics
Naval Postgraduate School
Monterey, California USA

September 13 - 15, 1978
STRESA - ITALY

Associazione Italiana di Aeronautica ed Astronautica

Associazione Industrie Aerospaziali

UNSTEADY AERODYNAMICS OF A CIRCULATION CONTROLLED AIRFOIL

Abstract:

The prime goal of the experimental results reported herein was the evaluation of the unsteady aerodynamics, and in particular, the transfer functions applicable to the Circulation Control Airfoil (CCA) for the situation of harmonic blowing perturbations superimposed upon a mean cavity pressure. Circulation control was achieved upon the relatively thick (t/c = 0.214) elliptically shaped two-dimensional airfoil by tangential jet injection at an upper surface slot just ahead of the rounded trailing edge.

The experiments were conducted in the Naval Postgraduate School 2.0 x 2.0 foot (0.61 x 0.61 m.) boundary layer wind tunnel. Preliminary results were obtained disclosing the nature of unsteady surface pressures over the airfoil, both amplitude and phase, relative to the oscillating cavity pressure for a range of reduced frequencies, k = 0 to 0.46, at a model attitude approximating the zero lift condition (blowing-off) at a moderate value of average momentum blowing coefficient. Positive results were obtained towards identifying the behavior of the Coanda sheet dynamics, airfoil lift transfer function and airfoil damping moment.

Nomenclature:

c	airfoil chord
C_C	airfoil chord force coefficient
C_L	airfoil lift force coefficient, Lift/qS
C_N	airfoil normal force coefficient
C_m	airfoil pitching moment coefficient, Moment/qSc
C_p	static pressure coefficient, $\Delta p/q$
C_μ	momentum blowing coefficient, $\dot{m}V_j/qS$
f	frequency, Hz
g	slot gap
G_x	gain function for variable "x", $G_x(f) = 1$ at $f = 0$
i	imaginary quantity, $(-1)^{\frac{1}{2}}$
k	reduced frequency, $\omega c/2V$
$\dot{m}$	jet mass flow rate, dm/dt
p	static pressure, $p(x,y,T)$
q	tunnel dynamic pressure, $\frac{1}{2}\rho V^2$
Re	Reynolds number, Vc/ν
S	wing area
t	airfoil thickness
T	time, sec
x	airfoil chordal variable, x = 0 at leading edge

y	airfoil ordinate
α	geometric angle of attack of CCA chord plane
ρ	density
ν	kinematic viscosity
ϕ_x	phase angle of variable "x", $\phi_x(f)$
ω	circular frequency, $2\pi f$
Δ	increment or incremental change

1. Introduction:

The term of Circulation Controlled Airfoil (CCA) refers to the lift generating mechanism achieved by tangential jet blowing that is injected at an upper surface slot just ahead of the rounded trailing edge of an elliptically shaped two-dimensional airfoil. The tangential jet forms a Coanda sheet which is predominantly a viscous flow dependent region. The remainder of the airfoil is influenced primarily by potential flow considerations including those associated with angle of attack, camber and more importantly by the location of the rear stagnation or separation point which is regulated by the level of tangential blowing, which in turn controls the Coanda sheet departure region. It is the latter influence which gives rise to the generic description of "circulation control".

The CCA concept, a form of boundary layer control, is competing for a multitude of high-lift applications in much the same manner as blown flaps and jet flaps. A complete literature survey and review of the properties of the CCA has been recently treated by Wilkerson, Ref. 1. Candidate aerodynamic applications of the CCA include: a.) fixed-wing STOL; c.f., Loth, Fanucci and Roberts, Ref. 2 and Englar, Ref. 3, b.) helicopter rotors; c.f., Cheeseman and Seed, Ref. 4 and Reader and Wilkerson, Ref. 5, and c.) stopped-rotor aircraft; c.f., Williams, Ref. 6. Since one of the applications of the CCA principle is to a rotorcraft where the rotor blade lift (or circulation) is cyclically adjusted in synchronization with blade azimuthal position by modulating the airfoil cavity pressurization, a logical item of technical concern and interest is the definition of the airfoil's aerodynamic performance in the context of a transfer function or frequency response.

The dominant factor in the CCA lift performance is the sensitivity of the airfoil to changes in jet momentum blowing coefficient, C_μ. The augmentation ratio of the airfoil $(\partial C_L / \partial C_\mu)$ may be viewed as the production of lift (coefficient) per unit of jet momentum blowing (coefficient) and local values of augmentation ratio in excess of 30 to 50 are not uncommon for well designed airfoils. The above concept of augmentation ratio usually applies to steady-flow situations in a local sense since the complete aerodynamic performance map, Ref. 1, usually discloses nonlinear features. In the context of this paper, airfoil operation will be considered in the neighborhood of a linear region and the augmentation ratio will have an interpretation as the D.C. (or static) gain of an aerodynamic amplifier. It is the purpose of the studies described herein to extend the aerodynamic

considerations of the CCA by investigating the unsteady aerodynamic behavior when harmonic blowing perturbations are superimposed upon a mean value of cavity pressure, and more specifically, to attempt an identification of these unsteady traits by aerodynamic transfer function considerations.

2. Background:

The conceptual arrangement of the CCA may be seen in Fig. 1 including the provision for an external air supply that provides pressurization to the airfoil cavity. The cavity may be considered as a reservoir operating at stagnation conditions. It is the mass flow leakage through the tailored slot that creates the Coanda sheet which is initially attached to the rounded trailing edge. The strength of the jet blowing is measured by the jet momentum coefficient, C_μ. A physical meaning may be attached to C_μ by recognizing that it is a dimensionless force coefficient and is directly equivalent to a lift coefficient if the jet were applied in the vertical direction from a body and no other source of lift were developed on the body. The ability of the CCA to generate lift increments in excess of 30 times the value of jet momentum blowing coefficient naturally leads one to consider the action as being analogous to an efficient aerodynamic amplifier. The lift due to Coanda blowing on a two-dimensional airfoil that is immersed in a uniform free-stream flow is illustrated on Fig. 1 as typically occurring in the mid-chord region.

In developing the concept of an aerodynamic transfer function, one naturally considers the frequency dependence of an output variable such as surface pressure, total airfoil lift or airfoil pitching moment relative to a prescribed input variable. It would seem reasonable to consider the input variable as being the unsteady jet momentum blowing coefficient when it is varying in a harmonic manner. A difficulty arises though because the determination of C_μ is based upon knowing the mass flow rate and jet exit velocity at the slot. While the mass flow rate can be directly measured in a steady environment, the jet exit velocity is dependent upon using compressible gas relations for isentropic, steady flow and consequently is an indirect measurement. In any event, the physical information required to determine the C_μ coefficient is not rigorously available in an unsteady situation.

It is not difficult to show that there is an approximate linear relationship between cavity pressurization level and C_μ for steady operation at moderate values of jet momentum blowing coefficient (see Fig. 2). By this reasoning, the upper portion of Fig. 2 depicts the manner that the lift coefficient due to circulation control tracks the cavity pressurization level. The quasi-steady behavior of lift production due to cavity pressure perturbations is depicted in Fig. 2 by the solid line between the triangle symbols (▲) and averaged about the mean value (⊙). The dashed line on Fig. 2 represents the trajectory of C_L vs. C_μ for an assumed situation of a 90 percent amplitude attenuation and 30 degree phase lag relative to the same input pressure perturbations that created the quasi-steady behavior pattern. The effects of an aerodynamic transfer function become readily apparent in the context of a phase-plane trajectory whereas much of the

behavior becomes obscured when looking at time histories of the variables, also shown figuratively on Fig. 2.

In the material to follow, the aerodynamic transfer functions will be referenced to cavity pressure perturbations as the input variable, and will be normalized relative to perturbation amplitudes that would correspond to unit lift coefficient production in steady flow.

3. Experiment:

The Circulation Control Airfoil under investigation was a prototype section supplied by the Aviation and Surface Effects Division of the David W. Taylor Naval Ship Research and Development Center (DWTNSRDC). The geometry of the uniform, two-dimensional CCA was approximately as follows:

Chord:	c = 10.2 inches (25.9 cm.)
Thickness ratio:	t/c = 0.214
Airfoil section:	Elliptical with modified trailing edge
Camber:	3.3 percent circular arc
Trailing edge rad.:	r/c = 0.048
Slot location:	x/c = 0.955
Slot gap:	g/c = 0.0016; g = 0.016 inches (0.041 cm.)

The model was installed in the test section of the Naval Postgraduate School (NPS) 2.0 x 2.0 foot (0.61 x 0.61 m.) boundary layer wind tunnel such that it spanned the center of the 17.0 foot (5.18 m.) long test section. The pressure supply to the model incorporated a rotating ball valve in the supply circuit which made possible the superposition of variable frequency, harmonic pressure perturbations upon the mean cavity pressure level. The test section dynamic pressure for these investigations was set at approximately 10 psf, which corresponded to a freestream velocity of 92 fps (28.0 mps) and a model Reynolds number of 0.5 x 10+6 (based upon airfoil chord length). At this operating condition, momentum blowing coefficients of up to about 0.12 were possible using the available air supply.

54 static pressure orifices were provided in the airfoil midspan region plus several near to the side walls and one inside the pressure cavity. All pressure tubing was of the same length, namely 25.5 inches (64.8 cm.) of 0.033 in. I.D. (0.084 cm.), and was connected to two customized Scanivalves. Frequency response calibrations of the pressure sensor system disclosed approximately a flat frequency response in the frequency range of test interest and a smooth variation of phase shift with the 90 degree lag point occurring at approximately 70 Hz. The unsteady pressure measuring technique is due to Bergh, Ref. 7 and has been described by Johnson, Ref. 8.

Steady-flow properties for the CCA airfoil were obtained from the static pressure distributions in order to establish a zero frequency data basis. Results as reported by Lancaster, Ref. 9 and Kail, Ref. 10 may be highlighted as follows:

a. Lift augmentation ratio, the ratio of lift coefficient production to momentum blowing coefficient ($\partial C_L/\partial C_\mu$) has been observed as having a value of approximately 30 for several moderate angle of attack settings.

b. The center of pressure for lift augmentation has been ascertained as being located at the 54 percent chord point.

c. With tangential jet blowing, the pressure distribution over the rounded trailing edge had a smooth variation and did not show signs of separation bubbles as evident in earlier measurements prior to refurbishment of the injection slot.

d. Additional upper surface static pressure orifices at 0.50 and 0.75 chord, away from the midspan instrumented station, confirmed the relatively two-dimensional nature of the flow field in the dominant central span area of the CCA model.

Unsteady aerodynamic measurements were made for the situation of an unsteady cavity pressure perturbation superimposed upon a mean or average pressurization level. The nominal or mean value of momentum blowing coefficient was set arbitrarily at approximately C_μ=0.035 which corresponded to a nominal cavity pressurization level of about 89 psf above ambient static and a mean jet velocity at the slot of approximately 290 fps (88.4 mps). It was possible to modulate the oscillating perturbation about the mean with amplitudes up to approximately +/- 50 psf. These relatively large pressure amplitudes were required in order to produce oscillating surface static pressure variations that were distinctly evident above the background tunnel generated pressure noise.

At the model angle of attack of -5.0 degrees, the blowing-off situation corresponded approximately to the zero lift condition. A mean value of momentum blowing coefficient of C_μ = 0.035 resulted in an approximate mean or D.C. value of lift coefficient of C_L = 1.05. The mean value of lift coefficient, which was obtained by integration of the recorded values of D.C. surface static pressure, did not change appreciably when cavity pressures were harmonically modulated about the mean value at various amplitudes and frequencies of test interest. This feature of the test results provided additional credence to the linear nature of the model's aerodynamic behavior for the test conditions investigated.

As an aside, the frequency range of interest corresponding to typical rotorcraft applications would usually be considered as being bounded by a frequency value of k = 0.10. The upper value of test frequency, 16.0 Hz, corresponded to a reduced frequency value of k = 0.46 which was in excess of the normal range of interest. It should be noted that the high value of reduced frequency did serve a purpose by establishing data trends.

The unsteady analog signal information was recorded upon a one-inch magnetic tape recorder with one channel being committed to the analog "clock", namely the cavity pressure perturbation. Other data channels included the signal information from the two Scanivalves and the hot wire in the pressure supply line. The analog recording at one

operating condition of all the surface pressure information typically required 39 analog records of 30 second duration each. For the frequency range of test interest, all pressure systems had approximately the same transfer function between input and transducer. Therefore, the small dynamic corrections were not applied to the readings.

Signal processing results of the unsteady surface pressure data at frequencies of 4.1, 8.0, 11.9 and 16.0 Hz are presented in a normalized fashion inasmuch as it was not possible to conduct each constant frequency data set at exactly the same cavity pressure amplitude value. Therefore, the data were adjusted, based upon linearity assumptions, such that the cavity pressure amplitude corresponded to a value which would produce a lift coefficient of $C_L = 1.0$ if the frequency were zero. As will be noted in the results, this method of data normalization produced consistently reasonable relationships.

Digitizing of the analog signal recordings was made at a sample rate of 250 samples per second to yield 1000 samples (four seconds) of discretized data for each channel of information at essentially the same sampling instant. The four frequency settings yielded over a half million data points, which were processed using a resident microprocessor system. The harmonic information, pressure amplitude and phase angle relative to the cavity "clock" signal, was extracted from the digitized data sets using a simple cross-correlation algorithm involving the cosine and sine of $(2\pi f\, n\Delta T)$ that yielded appropriate Fourier coefficients for the unsteady static pressures. Second harmonic content in the signal was typically less than two percent. Appropriate numerical integrations over the airfoil chord yielded, as a final result, four aerodynamic transfer function values that described the unsteady nature of circulation control type of lift generation and also disclosed an aerodynamic damping moment.

4. Coanda Sheet Dynamics:

Hot-wire studies by Kail, Ref. 10, confirmed that the Coanda sheet formed by tangential jet blowing was composed of turbulent flow. Unsteady pressure data results are shown in a normalized form for the viscous dominated Coanda sheet region, Fig. 3. Both pressure coefficient amplitude and phase shift (relative to the cavity pressure "clock") are shown as a function of dimensionless surface length. An alternate scale showing angular coordinate relative to the slot is also shown since the trailing edge region closely approximated a circular arc. Although at first glance, Fig. 3 may appear "busy", facts to be noted include:

a. The normalized pressure amplitude variation in the Coanda sheet region is very similar to previously observed steady-flow traits. The pressure coefficient builds up in amplitude from the slot to a peak value followed by a decrease to a region near the chord plane where the sheet separated from the airfoil. As might be expected, the average location of the rear stagnation point was dependent upon the mean value of momentum blowing coefficient.

b. The pressure amplitude distribution did not show any significant dependence upon frequency, as evident by the cross-hatched curves.

c. At zero frequency, one would expect the phase angle of Coanda sheet pressures to lead (or lag) the cavity pressure by 180 deg. since a positive pressure perturbation in the cavity would increase the Coanda sheet tangential velocities, and hence lower the corresponding surface static pressures. Note that the 180 degree lead angle was lessened by frequency increase, but the phase angle shift was essentially uniform in the attached Coanda sheet region.

d. Near the flow detachment point, the phase angle rapidly changed to a value of approximately zero degrees since the pressure perturbations on the lower surface of the airfoil ahead of the Coanda sheet detachment point tended initially to be in phase with the cavity pressures. This aspect will be brought out again during discussion of Fig. 5. It is interesting to note that it was only in this region that the pressure wave had a significant second harmonic present, presumably due to the fact that a local static pressure orifice was exposed to the flow domain on either side of the (oscillating) Coanda sheet's rear stagnation point.

e. The phase angle variations along the airfoil surface ahead of the injection slot exhibited similar traits to the Coanda sheet phasings when frequency was varied. However, the exact surface variation in the neighborhood of the slot was not well defined, hence dashed curves were used where appropriate to denote a degree of curve fairing uncertainty.

The relatively constant variation of pressure signal phase shift in the turbulent Coanda sheet, combined with a trend that the pressure amplitude did not appear frequency dependent, leads one to consider other physical factors as contributing to the phase shift dependency upon frequency variations. A plot of phase shift vs. reduced frequency, Fig. 4, at a Coanda sheet station about 2.5 percent of chord distance downstream from the jet injection slot clearly disclosed that the phase shift behaved linearly with respect to frequency. Classical control theory would suggest that the Coanda sheet behavior was dominated by a Transportation Lag type of phenomena with a form of $\exp(-Ts)$. For this situation:

$$\text{Gain: } |G(f)| = 1 \quad \text{and} \quad \text{Phase: } \phi(f) = -2\pi f T$$

The slope of the phase shift curve, Fig. 4, provides an estimate of the Transport Lag time constant T as being approximately 0.0043 sec. The time lag may be related to an equivalent transport lag distance that might correspond to some measure of the physical laws governing the flow from a reservoir or supply source into a smoothly contracting two-dimensional slot. The scaling laws for the above situation are not well known as of this writing, hence it would seem premature to place a physical meaning to the transport lag distance. At the present time, the only technique for relating the jet flow velocity at the slot exit to reservoir conditions is dependent upon gas dynamic relationships for steady flow with empirical modifications added under the guise of orifice coefficient corrections.

5. Main Airfoil Results:

For sake of clarity, the relations used to establish the unsteady lift coefficient expressions will be stated. In general, an oscillating lift coefficient would be expressed relative to a physically significant time base. For the results reported herein, the time base was the harmonically varying cavity pressure perturbation signal. Typical expressions for the lift coefficient would take the form of either:

$$C_L \sin(\omega T + \phi_L) \qquad \text{or} \qquad C_L \cos(\omega T + \phi_L) \ .$$

Furthermore, it should be realized that a frequency dependence exists in a functional sense such that:

$C_L = C_L(\omega)$ = Amplitude of lift coefficient

$\phi_L = \phi_L(\omega)$ = Phase angle relative to a time base

The unsteady lift coefficient may be reexpressed to the form of:

$$\begin{aligned} C_L \sin(\omega T + \phi_L) &= \left[C_L \cos\phi_L\right]\sin\omega T + \left[C_L \sin\phi_L\right]\cos\omega T \\ \text{or} \\ C_L \cos(\omega T + \phi_L) &= \left[C_L \cos\phi_L\right]\cos\omega T - \left[C_L \sin\phi_L\right]\sin\omega T \end{aligned} \qquad ..(\ 1\ )$$

where

$C_L \cos\phi_L$ = In-phase lift contribution

$C_L \sin\phi_L$ = Out-of-phase lift contribution

The in-phase and out-of-phase lift coefficients were obtained from the pressure distribution information by first integrating the pressure distributions to establish the in-phase and out-of-phase normal and chord force coefficients followed by a suitable coordinate transformation from body to wind axes. Equation 2 below shows the expression that defines $C_N \cos\phi_N$. Similar expressions were employed to obtain $C_N \sin\phi_N$, $C_C \cos\phi_C$ and $C_C \sin\phi_C$.

$$C_N \cos\phi_N = \int_0^1 \left[(C_p \cos\phi_N)_{lwr} - (C_p \cos\phi_N)_{uppr}\right] d(x/c) \qquad ..(\ 2\ )$$

The coordinate rotational transformation was of the form:

$$C_L \cos\phi_L = (C_N \cos\phi_N)\cos\alpha - (C_C \cos\phi_C)\sin\alpha \qquad ..(\ 3\ )$$

Figure 5 illustrates the phase angle variation over the airfoil chord for both the upper and lower surfaces as the cavity pressure perturbation was oscillated at 16.0 Hz. For comparative purposes, one would expect the effect of the Coanda sheet upon surface static pressures at zero frequency to produce 180 and 0 degree phase angle for the upper and lower surfaces respectively. From Fig. 5, one may observe sizable phase shifts taking place for the situation of the Coanda sheet harmonically oscillating at 16.0 Hz, with up to an 80 degree (1.4 rad.) lag change (relative to zero frequency) occurring

on the forward portion of the airfoil. The phase angle variation defined a smooth curve over the airfoil chord with the exception of the phase angle "jump" across the front and rear stagnation points.

In the neighborhood of (x/c) = 1.0, the cluster of upper surface pressures exhibited a phase shift of approximately 155 degrees, with the 25 degree difference from 180 degrees reflecting the influence of transport lag phenomena upon the Coanda sheet pressures. Similarly, the cluster of lower surface pressure phase angles near to a zero degree value is an indication of the phase angle situation just forward of the Coanda sheet departure point which corresponds to the airfoil rear stagnation point.

Figures 6 and 7 show unsteady pressure distributions over the airfoil in the form of $C_p \cos\phi$ and $C_p \sin\phi$ vs. (x/c) respectively. The pressure amplitudes, as stated previously, reflect normalization corrections using the cavity pressure perturbation amplitude such that the lift coefficient would be unity at zero frequency. The presence of the tangential jet blowing and the Coanda sheet is evident in the trailing edge regions by local curve "peaking". However, the leading edge pressure "peaking" from circulation control is not evident in Fig. 6, partially due to the influence of the cosine term.

Integration of the areas described by the curves of Figs. 6 and 7 yielded estimates as follows:

$$C_N \cos\phi_N = 0.569 \qquad \text{and} \qquad C_N \sin\phi_N = -0.444$$

Similar integrations for chord force coefficients yielded estimates:

$$C_C \cos\phi_C = 0.129 \qquad \text{and} \qquad C_C \sin\phi_C = -0.057$$

Application of eqn. 3 for an angle of attack of -5.0 degrees provided the result, in a normalized form, that the in-phase and out-of-phase lift coefficients were:

$$C_L \cos\phi_L = 0.578 \qquad \text{and} \qquad C_L \sin\phi_L = -0.447 \qquad ..(4)$$

Continuing the example further, one may obtain the magnitude and phase of the lift coefficient quite readily using the information of eqn. 4. Note that since the results were normalized to a unit value of lift coefficient at zero frequency, the C_L amplitude may then be viewed as a gain term in the aerodynamic transfer function for lift.

$$C_L = \left[(C_L \cos\phi_L)^2 + (C_L \sin\phi_L)^2 \right]^{1/2} = 0.731$$

and

$$\phi_L = \tan^{-1} \left[(C_L \sin\phi_L)/(C_L \cos\phi_L) \right] = -37.7 \text{ degrees} \qquad ..(5)$$

The result of eqn. 5 may be found plotted on Fig. 8 with the symbol (∇) as a function of the reduced frequency value corresponding to 16.0 Hz. Figure 8 represents the <u>first</u> experimental results of the aerodynamic lift transfer function due to unsteady circulation control about a mean (or average) momentum blowing coefficient of $\overline{C\mu} = 0.035$.

The lift transfer function, which is in general a complex natured quantity, is defined by:

$$G_L(k) = \frac{|C_L(k)|}{C_L(k=0)} \exp(i\,\Phi_L) \qquad ..(6)$$

General features apparent from the aerodynamic lift transfer function curve, Fig. 8, are that increasing the frequency produced a gradual attenuation in gain and a smooth growth in phase lag. It is a temptation to compare these results with a classical control system that has a simple pole since the transfer function exhibits many of the attributes of a simple pole system. However, it should be borne in mind that these transfer function curves include, in a serial manner, the consequences of the Coanda sheet transfer function. Hence, until a clearer picture of the scaling laws for the Coanda sheet region of the airfoil becomes available, it might be premature to generalize too broadly.

As stated earlier, the steady blowing performance of the CCA disclosed that the center of pressure for circulation control generated lift was at approximately the 54 percent chord location for operation in the linear region. A similar type of description was sought for the unsteady pitching moment coefficient data. Analysis of the data disclosed that the in-phase and out-of-phase pitching moment coefficients did not concurrently vanish at any chordwise location. This fact suggested the presence of damping type terms in the unsteady pitching moment coefficient. Since frequency dependent terms should vanish at f = 0, the unsteady pitching moment coefficient at the (x/c) = 0.54 location was evaluated, Fig. 9. Conclusions to be noted from Fig. 9 include that:

a. The magnitude of pitching moment coefficient vanished as frequency went to zero.

b. The phase angle tended to -90 degrees as frequency went to zero.

The variation of amplitude with frequency is nonlinear, and suggests that an analytic expression for the unsteady moment might include terms that are dependent upon the reduced frequency, k, in much the same manner as in conventional airfoil unsteady aerodynamics.

6. Concluding Remarks:

An experimental technique has been established which allows the measurement of unsteady airfoil surface static pressures and subsequent digital data processing for the express purpose of defining aerodynamic transfer functions of Circulation Control Airfoils.

Recent results, Ref. 11, for the CCA model at one angle of attack, one tunnel airspeed, and harmonic oscillation of the cavity pressure at four frequency values using one average value of momentum blowing coefficient have been described. A summary of the results, some of which are original to these investigations, includes:

a. The airfoil behaved in a linear manner.

b. The mean or average value of lift coefficient was not altered during unsteady blowing.

c. The frequency response traits of the Coanda sheet region suggest the presence of transportation lag between the pressure cavity and the blowing slot.

d. The overall airfoil lift transfer function from harmonic circulation control variations had a behavior quite similar to that of a simple pole in classical control theory.

e. A frequency dependent pitching moment about the 54 percent chord center of pressure location for circulation control type lift was evident with the attributes of aerodynamic damping being shown.

Acknowledgments:

The results presented herein are due to the efforts of many individuals including Professor J.A. Miller, LTS(USN) Bauman, Englehardt, Kail, Lancaster and Picklesimer and staff members in the Department of Aeronautics, Naval Postgraduate School. However, the program could not have been accomplished without the trust and support of the principle sponsor, Mr. R.F. Siewert of the Naval Air Systems Command, AIR-320D, Washington, D.C.. The research is currently sponsored by Naval Air Systems Command contract N00019-78-WR-81002.

References:

1. J.B. Wilkerson, "An Assessment of Circulation Control Airfoil Development", DWTNSRDC Rep. 77-0084, August 1977.

2. J.L. Loth, J.B. Fanucci and S.C. Roberts, "Flight Performance of a Circulation Controlled STOL Aircraft", Jour. of Aircraft, Vol. 13, pp. 169-173, March 1976.

3. R.J. Englar, "Circulation Control for High Lift and Drag Generation on STOL Aircraft", Jour. of Aircraft, Vol. 12, pp. 457-463, May 1975.

4. I.C. Cheeseman and A.R. Seed, "The Application of Circulation Control by Blowing to Helicopter Rotors", Jour. R.Ae.S., Vol. 71, No. 848, July 1966.

5. K.R. Reader and J.B. Wilkerson, "Circulation Control Applied to a High Speed Helicopter Rotor", 32nd Annual National Forum of the AHS, Paper 1003, Washington, D.C., May 1976.

6. R.M. Williams, "Application of Circulation Control Rotor Technology to a Stopped Rotor Aircraft Design", DWTNSRDC Rep. 4574, December 1975.

7. H. Bergh, "A New Method for Measuring the Pressure Distribution on Harmonically Oscillating Wings", Proc. of the 4th ICAS Cong., Paris, 1964.

8. R.B. Johnson, LT(USN), "A Technique for Measuring Unsteady Pressures", M.S. Thesis, NPS, September 1968.

9. E.J. Lancaster, LT(USN), "Initial Unsteady Aerodynamic Measurements of a Circulation Controlled Airfoil and an Oscillating Flow Wind Tunnel", M.S. Thesis, NPS, June 1977.

10. K.A. Kail IV, LT(USN), "Unsteady Surface Pressure and Near-Wake Hotwire Measurements of a Circulation Control Airfoil", Eng. Thesis, NPS, September 1977.

11. L.V. Schmidt, "Circulation Control Airfoil Study, Progress Report No. 4", NPS Rep. 67SX-77111, November 1977.

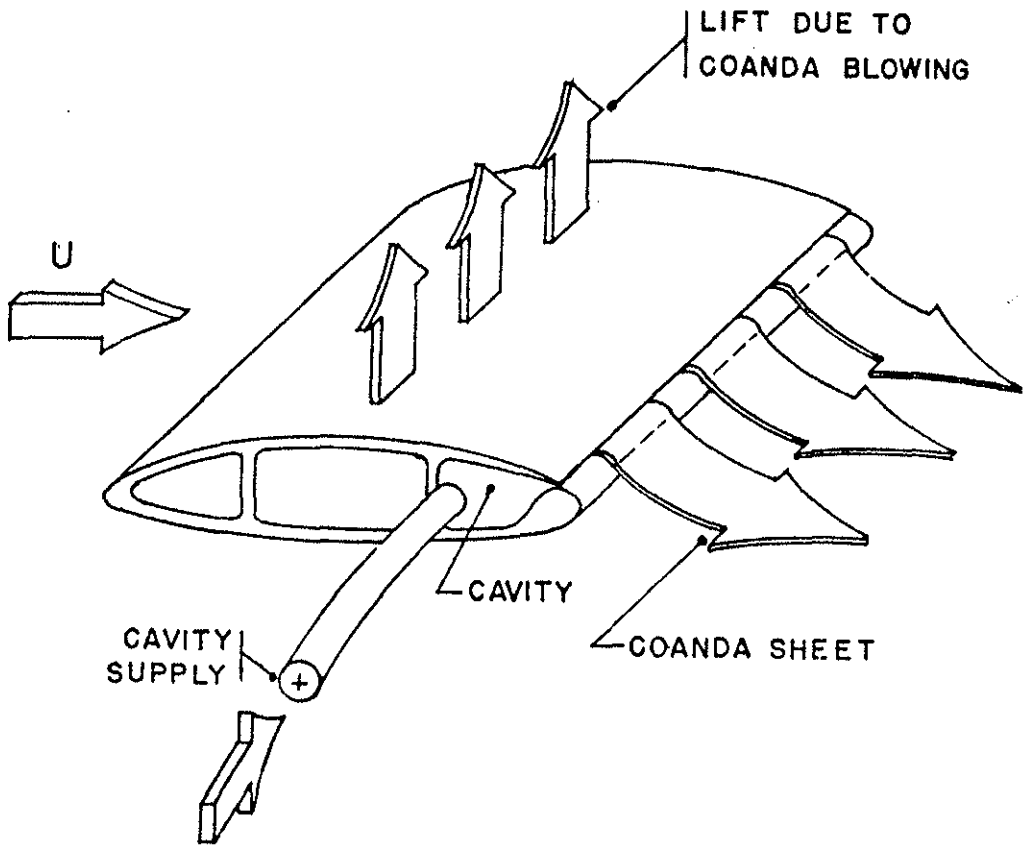

FIG. 1: SKETCH OF CIRCULATION CONTROL AIRFOIL

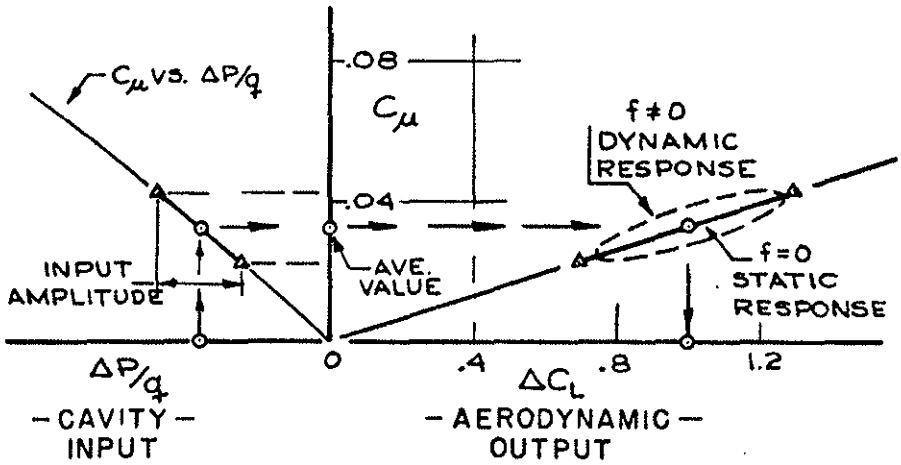

(a.) PHASE PLANE LIFT RESPONSE

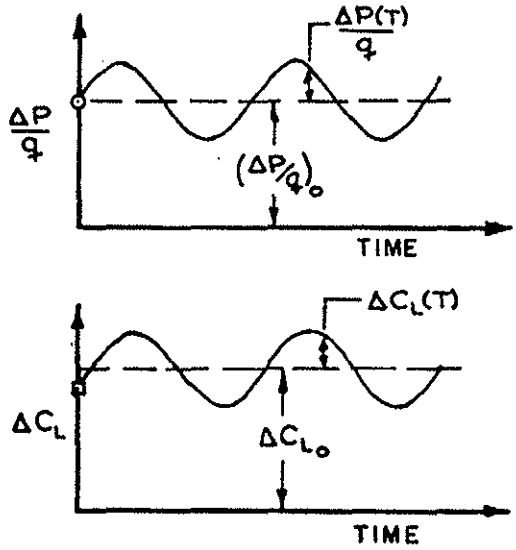

(b.) TIME HISTORY PLOTS

FIG. 2: SKETCH OF AERODYNAMIC RESPONSE

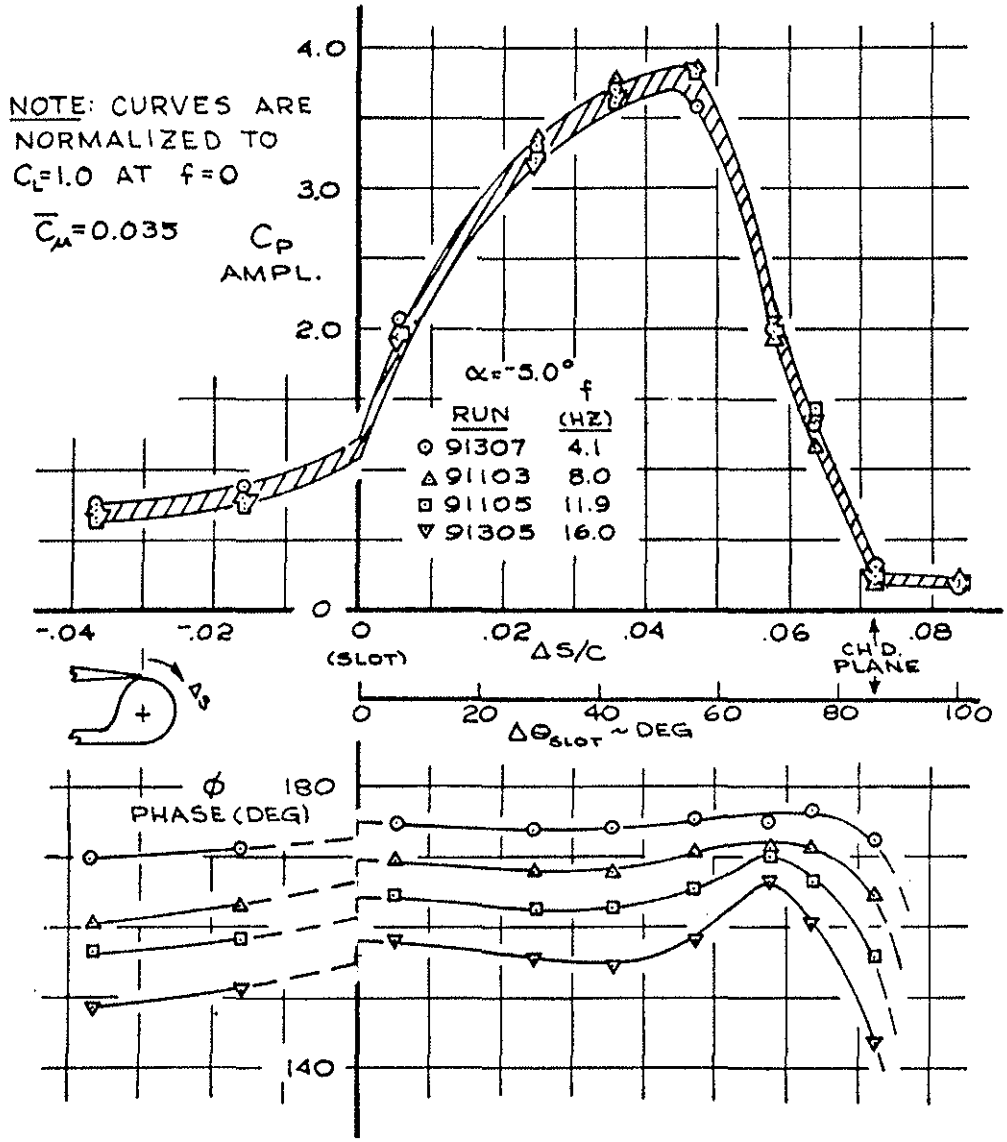

FIG. 3: COANDA SHEET PRESSURE DYNAMICS

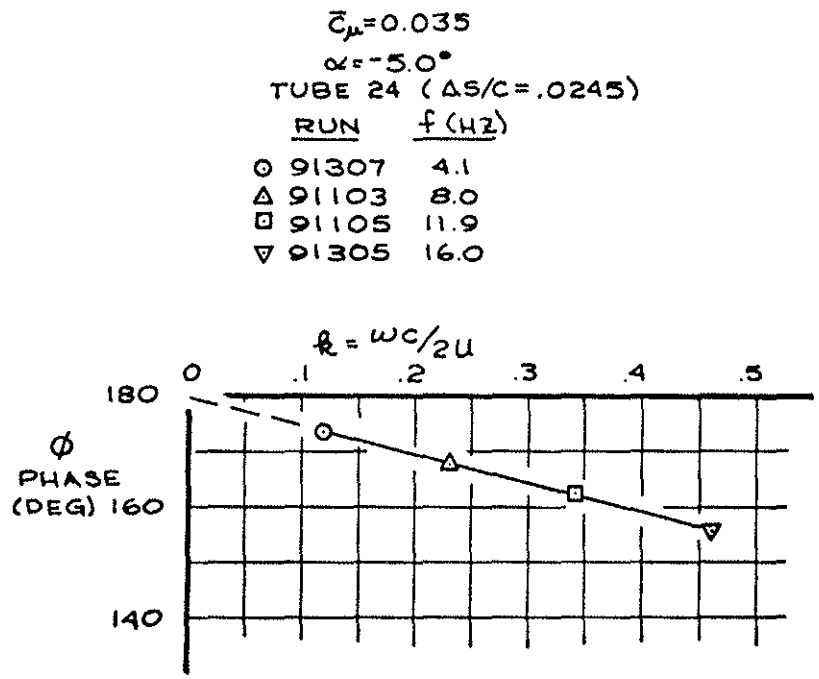

FIG. 4: COANDA SHEET PHASE LAG

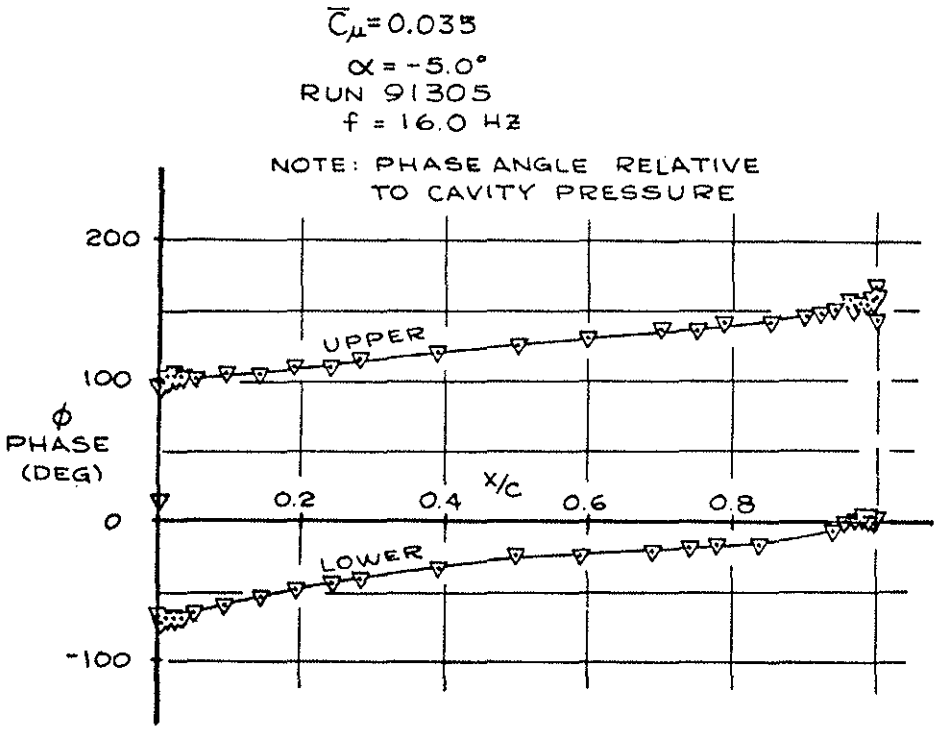

FIG. 5: AIRFOIL SURFACE PRESSURE PHASE ANGLES

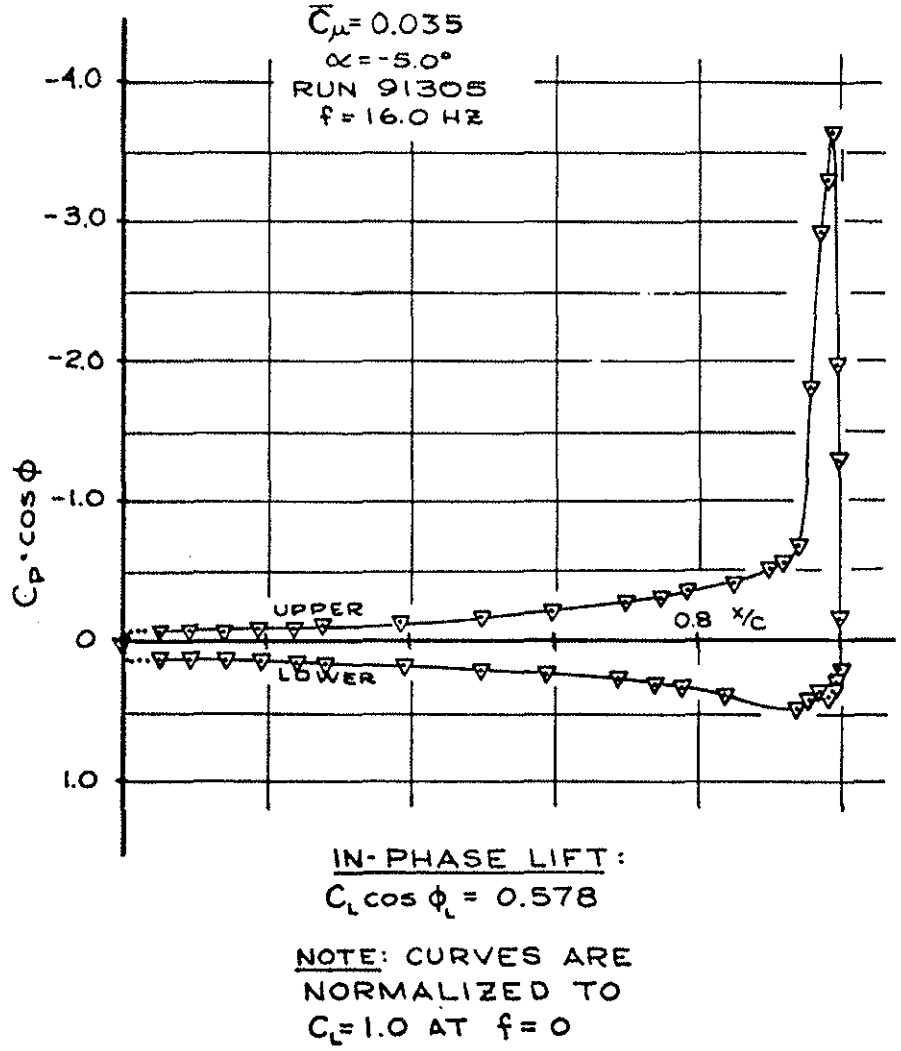

FIG. 6: AIRFOIL IN-PHASE PRESSURE DISTRIBUTION

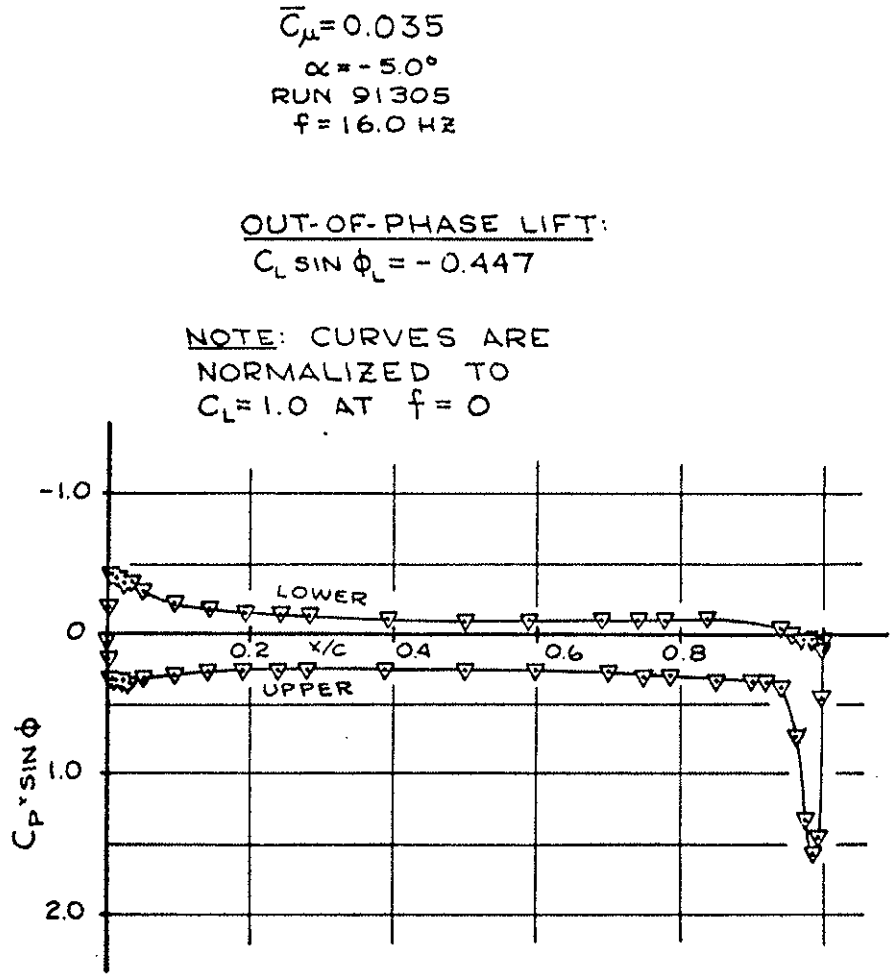

FIG. 7: AIRFOIL OUT-OF-PHASE PRESSURE DISTRIBUTION

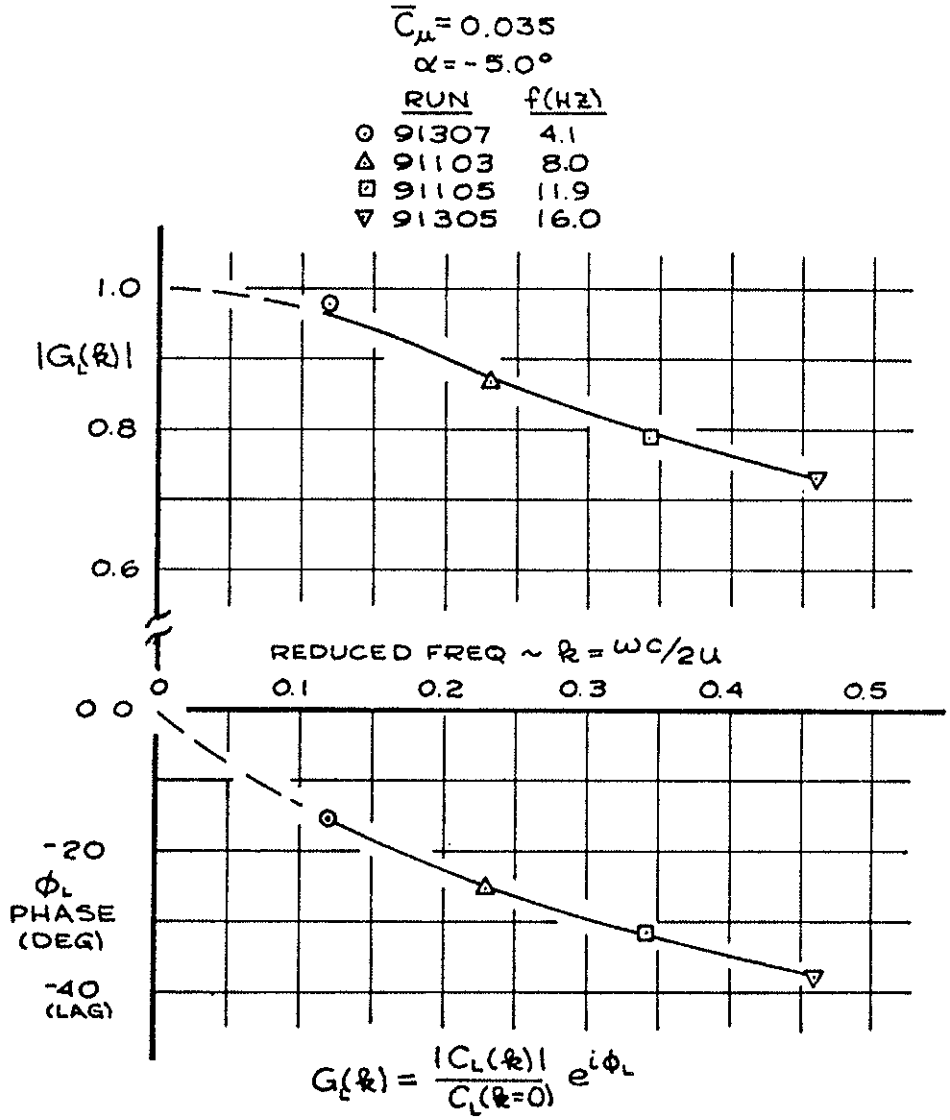

FIG. 8: CIRCULATION CONTROL LIFT TRANSFER FUNCTION

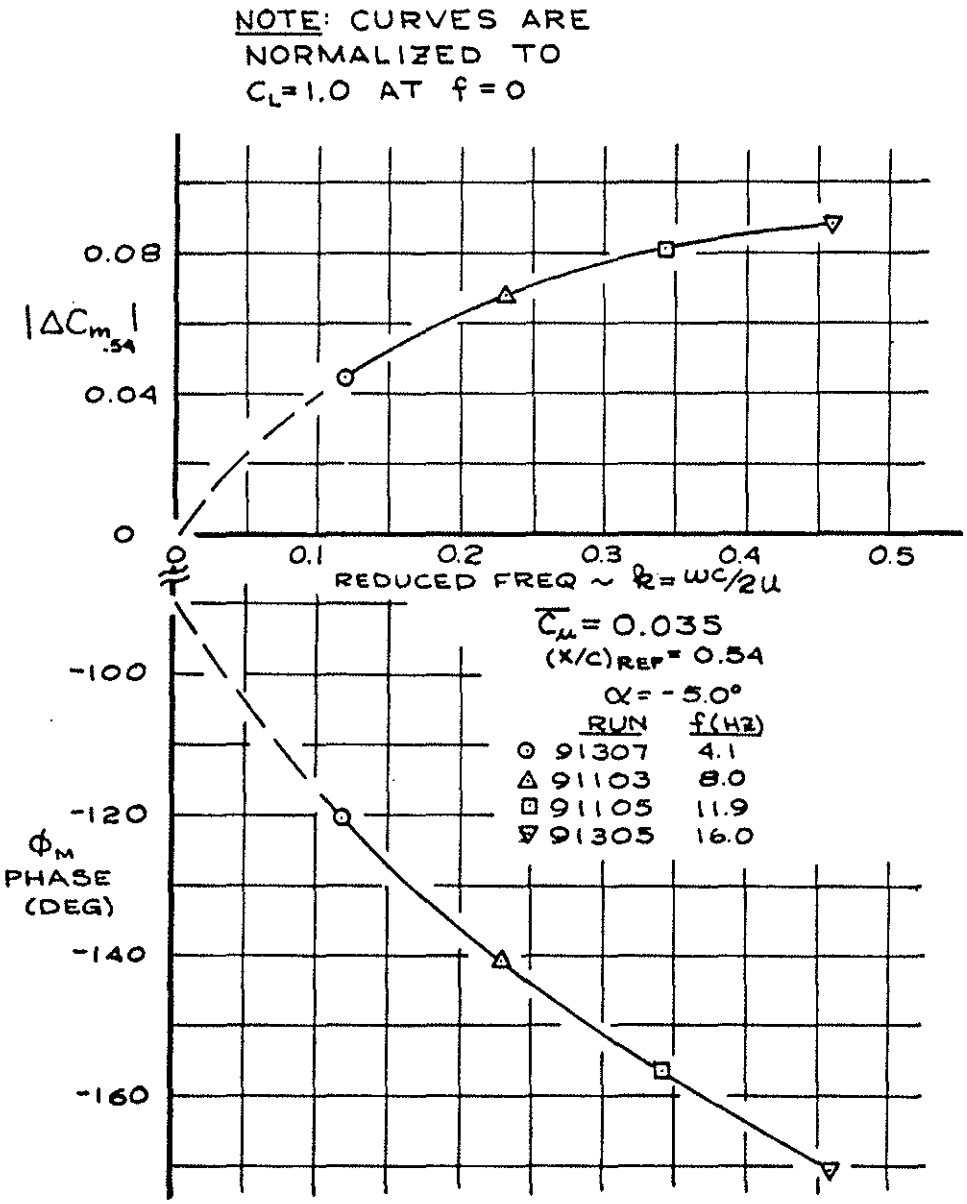

FIG. 9: PITCHING MOMENT DYNAMICS